Supplementary Information for

Victorin, the Host-Selective Cyclic Peptide Toxin from the Oat Pathogen *Cochliobolus victoriae*, is Ribosomally Encoded.

Simon C. Kessler[1,†], Xianghui Zhang[2,3†], Megan C. McDonald[4], Cameron L. M. Gilchrist[1], Zeran Lin[2], Adriana Rightmyer[2], Peter S. Solomon[4], B. Gillian Turgeon[2*], Yit-Heng Chooi[1*]

[1]School of Molecular Sciences, The University of Western Australia, Perth, WA 6009, Australia.
[2]Section of Plant Pathology & Plant-Microbe Biology, School of Integrative Plant Science, Cornell University, Ithaca, NY, 14853, USA.
[3]College of Plant Science, Jilin University, Changchun, China.
[4]Research School of Biology, The Australian National University, Canberra, ACT 2601, Australia.

[†] S.C.K. and X.Z. contributed equally to this work

* Corresponding authors: Yit-Heng Chooi and B. Gillian Turgeon

Email: yitheng.chooi@uwa.edu.au; bgt@cornell.edu

This PDF file includes:

www.pnas.org/cgi/doi/10.1073/pnas.2010573117

Supplementary Material and Methods

DNA sequencing and genome assembly. High molecular weight DNA of *C. victoriae* strain FI3 was prepared and sequencing was performed on Oxford Nanopore's MinION sequencer. R9.4 flow cells were used for sequencing and the 1D library kit SQK-LSK08 was used to prepare the libraries according to the manufacturer's protocol. All DNA samples were purified using Agencourt AMPure beads prior to starting the 1D library preparation (Beckman coulter, Inc. CA, USA). Genomes were assembled with Canu v1.5 with a minimum read length of 5 kb [1]. *De novo* genome assemblies were corrected using the trimmed reads output from Canu. Trimmed reads were mapped to the genome with Minimap2 followed by correction with Racon [2]. The output consensus sequence from Racon was used as input for additional corrections steps performed iteratively up to five times. The assembly was further refined using the software Pilon, this correction was also performed iteratively up to five times [3]. Illumina data from for *C. victoriae* FI3 isolate were downloaded from JGI Mycocosm (https://mycocosm.jgi.doe.gov/Cocvi1/Cocvi1.home.html).

Whole chromosome alignment and repeat annotation. Initial whole chromosome alignments (WCA) were conducted using Lastz v1.02.00 or Mauve as implemented in Geneious v.9.1.8. WCA of the chromosomes containing the precursor peptide genes was performed with LASTZ with the following settings:--entropy --format=general:name1,strand1,start1,end1,length1,name2,strand2, start2+,end2+,length2,score,identity --markend --gfextend --nochain --gapped --step=1 --strand=both --output=Tig12_tig32_out_nogap.txt --identity=70 --continuity=80 --matchcount=1000. This output was filtered for alignments greater than 2 kb in length and 80% nucleotide identity and used as input for plotting in R. Chromosomal alignments were plotted in R v3.5.2 using the package genoPlotR [4].Transposons and repetitive sequences were identified *de novo* using the TEdenovo pipeline distributed as part of the REPET package v2.5 [5, 6]. TEs were collapsed in a non-redundant library using the RemoveRedundancyBasedOnCI.py script available from the REPET developers. Finally, TEs and repeats were annotated following the TEannot pipeline.

Gene annotations and gene density analysis. Gene annotations were transferred from the JGI *C. victoriae* FI3 genome assembly and manually curated in the *Vic1* and *Vic2* loci using Geneious version 7.1.9 and the AUGUSTUS plugin [7]. SignalP 5.0 was used to predict signal peptide sequences of precursor peptides [8]. Protein sequence alignments shown in Tables S2, S3 and S4 were performed in Geneious version 7.1.9 using MUSCLE with default settings.
Gene density analysis of the *C. victoriae* genome was performed using custom Python scripts. Briefly, gene features were extracted and 5' and 3' intergenic distances were identified by taking the distance (in base pair) between every gene and their immediate upstream and downstream neighbors. Genes on contig edges were omitted. Intergenic distances were then plotted to visualize gene density of the *C. victoriae* genome. All code used in this analysis is available in a Jupyter notebook, which is available at: https://github.com/gamcil/C_victoriae_gene_density.

Construction of gene deletion strains. Candidate genes were deleted using the split-marker method [9] and the transformation protocol described earlier [10]. All primers were designed using Gene Runner 3.05 and 4.0.9.3 Beta software, Primer3 plus software and Geneious version 7.1.9. Primers for deletion are listed in Table S6 and all strains used or constructed in this study are listed in Table S5. The 5' and 3' flanking sequences of each target sequence to be deleted were amplified from DNA of WT strain FI3, using two specific primer sets that matched the upstream and downstream sequences (Figs. S4 and S5, Table S6). These products along with the *hygB* cassette (*HYG*) amplified from pUCATPH [11], which confers resistance to hygromycin B [12] were added to protoplasts. PCR amplification of transformation constructs was carried out with iProof high-fidelity DNA polymerase (Bio-Rad, Hercules, CA, U.S.A), following the manufacturer's instructions. For *vicA,* after deletion of a first gene copy, a verified *vicAhygB*^{R} transformant (Δ*vicA**-2, Table S5, Fig. S4) was selected for a second round of deletions. A second selectable marker, *NPTII,* which confers resistance to G418, was used to delete another copy of *vicA,* this time targeting the internal region within the boundaries that had been deleted in the first round. For *vicYb, vicK,* and *NOX5,*

the predicted ORFs of each gene were completely deleted and replaced with the *hygB* cassette as described above (Fig. S5, Table S5).

PCR verification of gene deletion. All PCR amplifications for confirmation of gene deletion were conducted with GoTaq polymerase (Promega Corp., Madison, WI, U.S.A.). Deletion was verified using three diagnostic primer sets as described previously [13] (Table S6, Figs. S4 and S5). One set of primers (F/R) amplified an internal region of the target gene; a PCR product is expected from WT and ectopic transformants but should be missing from single copy gene deletion mutants. Because there are three copies of *vicA*, if one or two copies are deleted, primers F/R will detect the remaining copy. The two additional primer sets confirm correct insertions into the 5′ and 3′ regions flanking the target gene. For these, a specific primer matching sequence outside the 5′ or 3′ flanking sequences used for deletion and a primer in the *hygB* gene (U/NLC37 or NLC38/D, respectively) were used (Fig. S4). Only targeted deletion strains yield a PCR product; these bands will not be present in WT or ectopic strains [13]. For double *hygB*^{R}*nptII*^{R} *vicA* mutants, the foregoing primers will verify that the *hygB* gene inserted into a copy of *vicA*; these bands will be amplified from both single and double *vicA* mutants. Primers U/DW70 and DW69/D will verify that *NPTII* inserted into a second copy of *vicA*. Only double mutants will amplify these bands (Fig. S4).

Mass spectrometry. For MS^1 analysis an Agilent 1260 liquid chromatography with a Kinetex C18 column (2.1 x 100 mm, 2.6 µm), coupled to an Agilent 6130 Quadrupole mass spectrometer with an ESI source was used. The mobile phase was a 10 min linear gradient of 5 – 95% acetonitrile-water containing 0.1% formic acid. Agilent MassHunter Qualitative Analysis version B.07.00 was used for LC-MS data analysis.
MS^2 analysis was performed on a Thermo Scientific Fusion Orbitrap coupled to a Thermo Ultimate 3000 UHPLC. The column used was an Agilent Poroshell 120 SB-C18 (2.1 x 100 mm, 2.7 µm) with a 20 min linear gradient of 5 – 95% acetonitrile-water containing 0.1% formic acid. Fragmentation was achieved with higher-energy collisional dissociation (HCD) at a normalized collisional energy value of 22, 25 and 28% (stepped collision energy). Thermo Scientific FreeStyle version 1.3 was used for LC-MS/MS data analysis. HighChem Mass Frontier 8.0 was used for LC-MS/MS fragmentation predictions.
The mass error of the obtained data was calculated from different polysiloxane peaks ($[M+H]^+$, $[M+NH_4]^+$ and $[M+H-CH_4]^+$ ions of $[C_2H_6SiO]_6$, $[C_2H_6SiO]_7$ and $[C_2H_6SiO]_8$) [14]. MS^2 data were re-calibrated with Thermo Fisher RecalOffline 4.1.2 using the theoretical mass of $[M+H]^+$ ion of $[C_2H_6SiO]_8$ (m/z = 593.1576).

Preparation cell-free lysate and purification of HV-toxin M for *in vitro* oxidative deamination. To obtain **3** in sufficient quantities, multiple Δ*vicK1/2* cultures were set up and victorin was extracted as described above. Extractions were combined and further purified on the Agilent 1260 liquid chromatography with a Vydac Denali C18 column (10 x 250 mm, 5 µm). Acetonitrile was evaporated from collected fractions and the remaining aqueous solutions were checked for the presence of **3** and the absence of **1** by LC-MS. Fractions without **1** but containing **3** were combined and used as substrate for the assay.
vicK was amplified by PCR from *C. victoriae* FI3 gDNA with the primer pair PalcS-vicCOX-F/T1-vicCOX-2R (Table S6). *vicK* was inserted into the hybrid yeast-fungal artificial chromosome expression vector pYFAC [15] containing the *pyrG* marker by Gibson Assembly [16], with *vicK* expression under control of the alcohol inducible promotor *alcS* [17]. The assembled plasmid was used to transform *A. nidulans* strain LO8030 by polyethylene glycol-mediated protoplast transformation as described previously [18]. About 10^8 spores/L from a transformant were used to inoculate 500 ml of glucose minimal medium supplemented with pyridoxine and riboflavin. Cultures were incubated at 37 °C and 200 RPM for 18 h, gene expression was induced by addition of 2.5 ml/l cyclopentanone and then kept at 25 °C and 180 RPM for 2 d. Mycelium was harvested, frozen, ground with mortar and pestle, re-suspended in 50 mM Tris-HCl pH 7.5 and lysed by sonication. Cell debris was removed by centrifugation and the supernatant was used for *in vitro* assays.

Growth media. Modified Fries medium [19]: 5 g ammonium tartrate, 1 g NH_4NO_3, 1 g $MgSO_4 \cdot 7H_2O$, 0.1 g NaCl, 0.1 g $CaCl_2$, 30 g sucrose, 1 g yeast extract and 1 ml iron solution per liter. Iron solution: 20 g $FeSO_4 \cdot 7H_2O$ and 24.1 g EDTA per liter, autoclaved.
Complete medium (CM or CMX) [20, 21]: 10 ml solution A, 10 ml solution B, 0.5 ml Srb's micronutrients, 1 g yeast extract, 0.5 g acid-hydrolyzed casein, 0.5 g enzymatically hydrolyzed casein, 10 g glucose for CM or 10 g xylose for CMX, 20 g agar per liter, autoclaved. Solution A: 100 g $Ca(NO_3)_2 \cdot 4H_2O$ per liter, autoclaved. Solution B: 20 g KH_2PO_4, 25 g $MgSO_4 \cdot 7H_2O$, 15 g NaCl per liter, pH 5.3, filter sterilized. Srb's micronutrients: 57.2 mg H_3BO_3, 393 mg $CuSO_4 \cdot 5H_2O$, 13.1 mg KI, 60.4 mg $MnSO_4 \cdot H_2O$, 36.8 mg $(NH_4)_6Mo_7O_{24} \cdot 4H_2O$, 5.49 mg $ZnSO_4 \cdot H_2O$ and 948.2 mg $FeCl_3 \cdot 6H_2O$ per liter, autoclaved.
Glucose minimal medium [22]: 10 g Glucose, 6g $NaNO_3$, 1.52 g K_2HPO4, 0.52 g KCl, 0.52 g $MgSO_4 \cdot 7H_2O$, 22 mg $ZnSO_4 \cdot 7H_2O$, 11 mg H_3BO_3, 5 mg $MnCl_2 \cdot 4H_2O$, 1.6 mg $FeSO_4 \cdot 7H_2O$, 1.6 mg $CoCl_2 \cdot 5H_2O$, 1.6 mg $CuSO_4 \cdot 5H_2O$, 1.1 mg $(NH_4)_6Mo_7O_{24} \cdot 4H_2O$ and 50 mg Na_4EDTA per liter, pH 6.5, autoclaved.

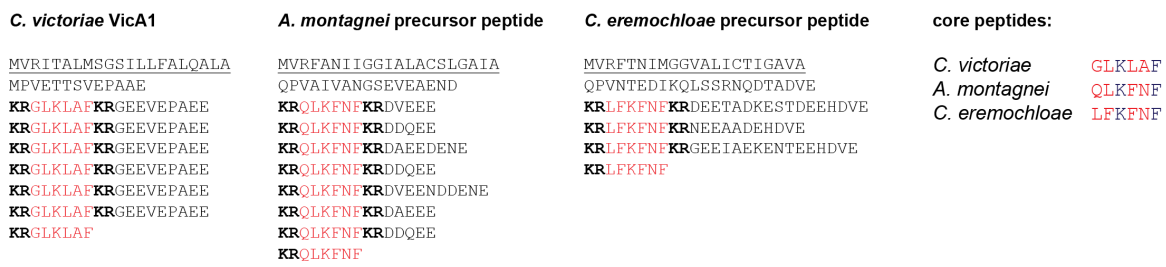

Figure S1. Comparison of victorin precursor peptide VicA1 to homologs found in the genomes of *A. montagnei* and *C. eremochloae*. The signal peptide is underlined, putative kexin recognition sites are shown in bold and the core peptide is shown in red. Alignment of VicA core peptide with putative core peptides of VicA homologs on the right. Conserved amino acids shown in blue.

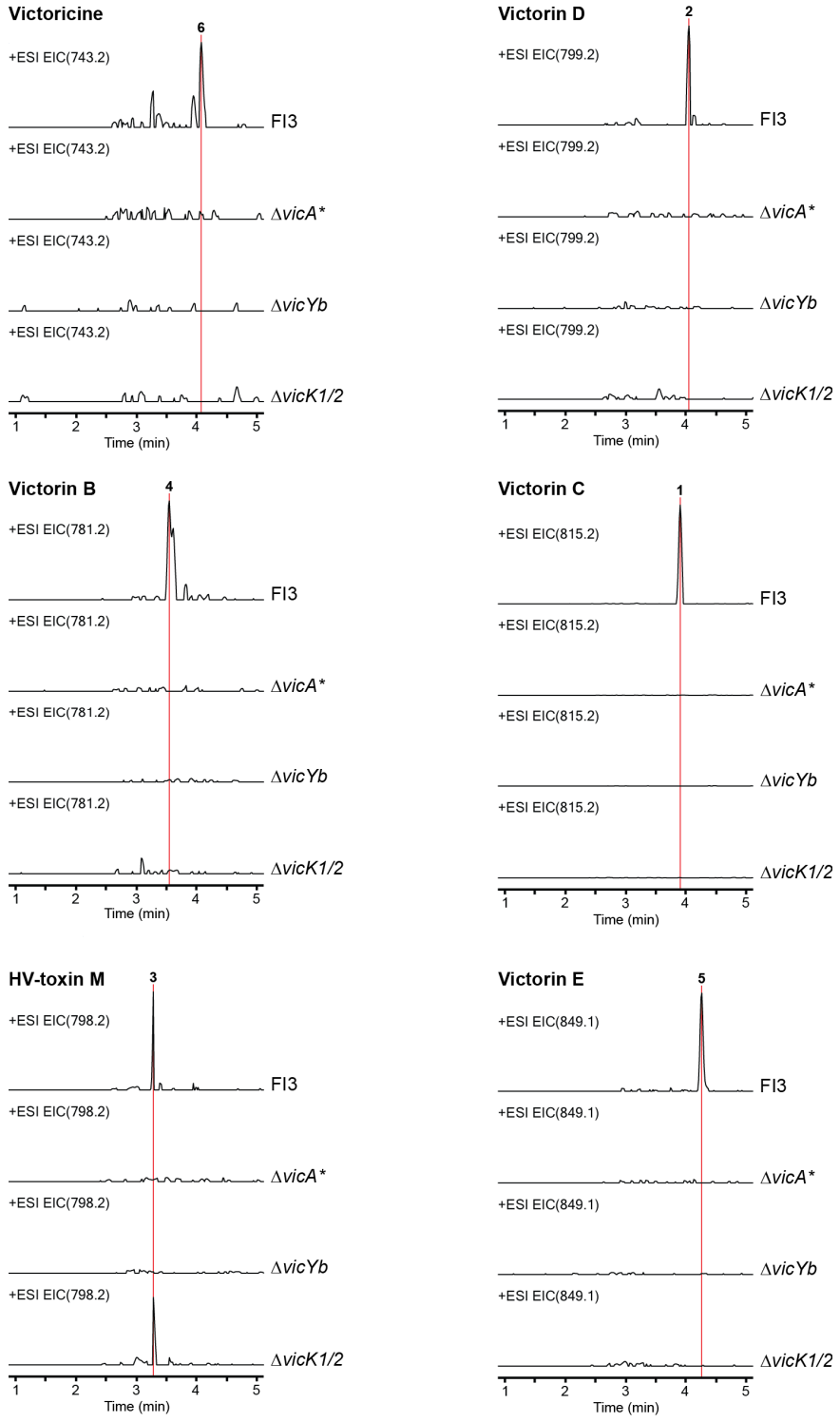

Figure S2. Victorin production LC-MS analysis of wild type strain *C. victoriae* FI3 and gene deletion mutants. EICs correspond to $[M+H]^+$ masses of victorin B, C, D, E, HV-toxin M and victoricine.

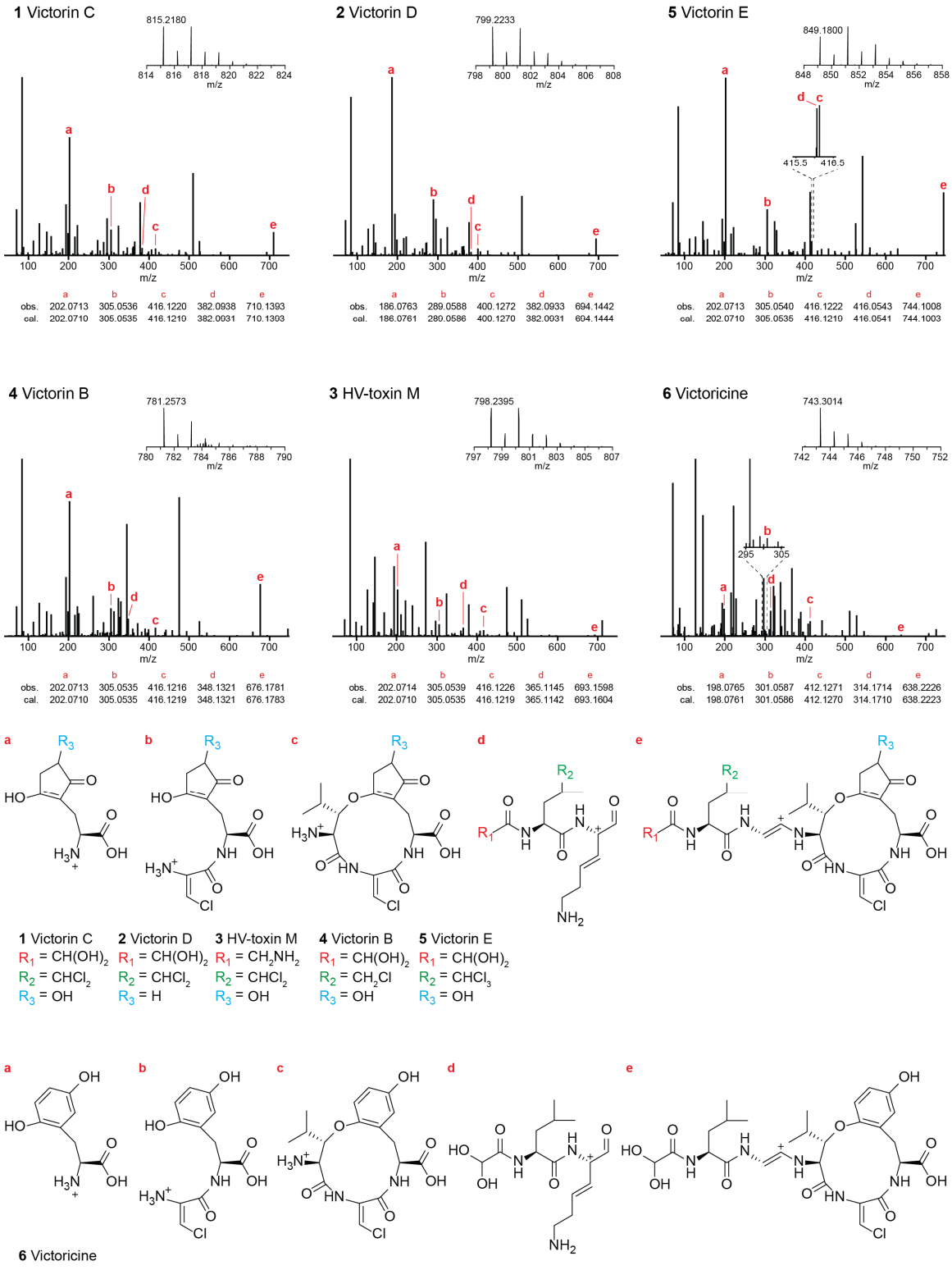

Figure S3. MS^2 analysis of *C. victoriae* FI3 culture filtrate. MS^1 and MS^2 spectra of $[M+H]^+$ ions corresponding to masses of victorin B, C, D, E, HV-toxin M and victoricine, with proposed structures of select fragments.

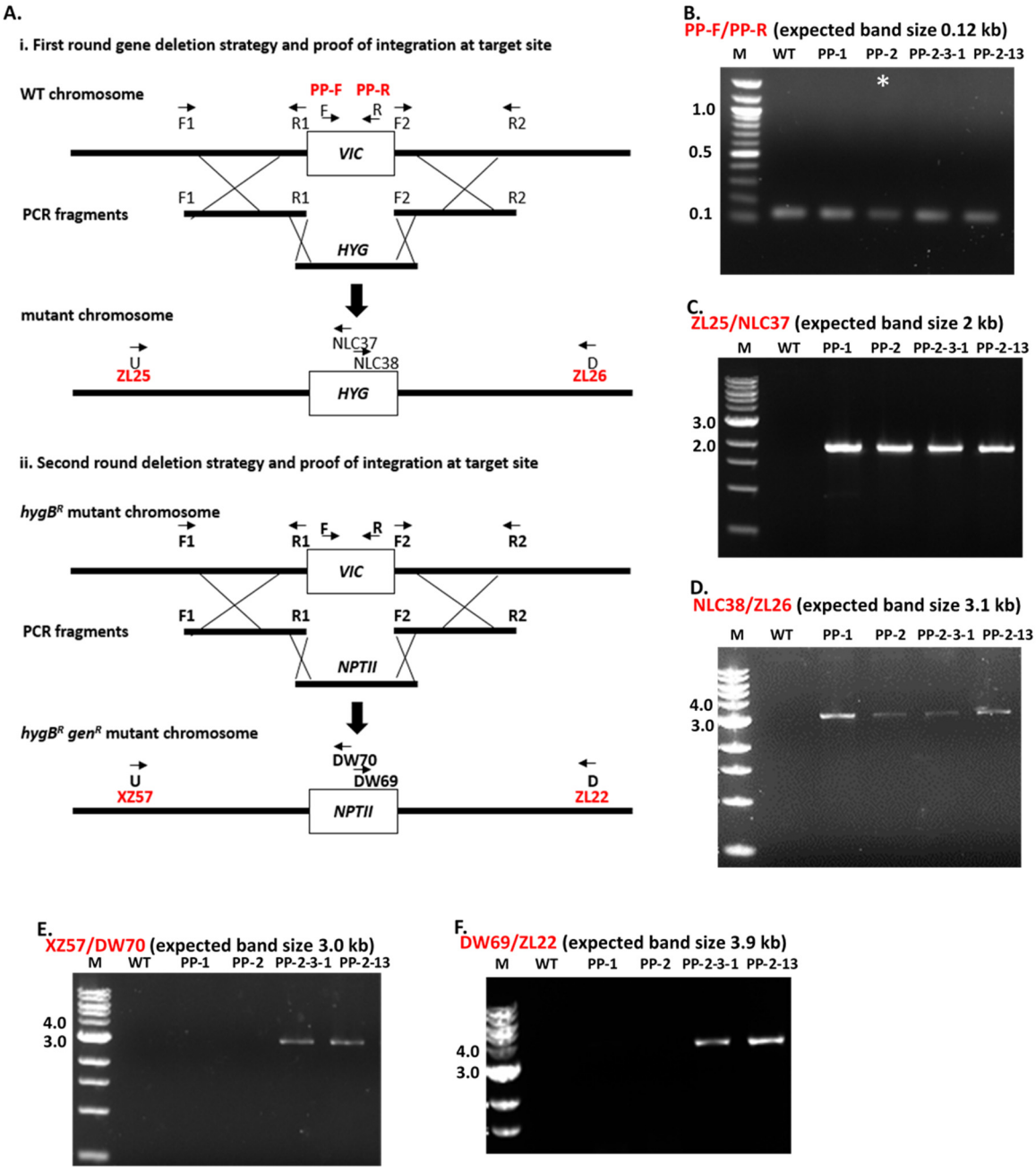

Figure S4. Gene deletion strategy and proof of integration at target site using the precursor peptide gene (*vicA*) as an example. Primers used are listed in Table S6.

For *vicA,* the entire coding region plus 150 bp upstream and 300 bp downstream of the tri-replicated *vicA* gene was targeted initially. Then the protocol was repeated using transformant (PP-2/Δ*vicA**) from this round, verified as below. In the second round, the fragment deleted in the first round was the target, so that a different copy of *vicA* was deleted.

A. Top: Gene deletion strategy. Primer pairs F1/R1 and F2/R2 were used to amplify the 5' and 3' flanking regions of the gene (*vicA*), respectively, from WT FI3 DNA and these products along with the *hygB* cassette (*HYG*) amplified from pUCATPH [11] were added to protoplasts. If correctly integrated, the gene was replaced by *HYG.* Diagnostic PCR screening strategy was used

to identify candidate gene-deleted transformants. Primer pairs U/NLC37 (ZL25/NLC37 for *vicA*) and D/NLC38 (ZL26/NLC38 for *vicA*) were used confirm that the selectable marker was inserted at the target site in the mutants. No product was expected when WT DNA was used as template. Primer pair F/R (PP-F/PP-R) confirmed presence/absence of the targeted gene in WT and mutants, respectively.

B. Diagnostic PCR with F/R (PP-F/PP-R) primers demonstrated that at least one copy of *VICA* remained after two rounds of transformation. Lanes, left to right: 100 bp marker, WT FI3, first round confirmed mutants PP-1, PP-2 (asterisk, *ΔvicA**), second round mutants, PP-2-3-1 and PP-2-13, constructed in strain PP-2 (*ΔvicA***). Note that the diagnostic internal *vicA* 0.12 kb band was still present in all strains.

C., D. Diagnostic PCR demonstrated that the *hygB* selectable marker inserted at the *vicA* target site. Lanes, left to right: as in **A**, except that the 1 kb marker was used. Note that bands of expected size were amplified in both single and double *vicA* mutants (ZL25/NLC37 = 2 kb, NLC38/ZL26 = 3.1 kb).

E., F. Diagnostic PCR demonstrated that the *NPTII* selectable marker inserted at the target site in *vicAhygB*^{R} progenitor mutant PP-2 (*ΔvicA**). Lanes, left to right: as in **A**, except that the 1 kb marker was used. Note that bands of expected size were amplified only in double *vicA* mutants PP-2-3-1 and PP-2-13 (XZ57/DW70 = 3 kb, DW69/ZL22 = 3.9 kb).

Similar protocols were used for deletion of *vicYb*, *vicK* and *NOX5*.

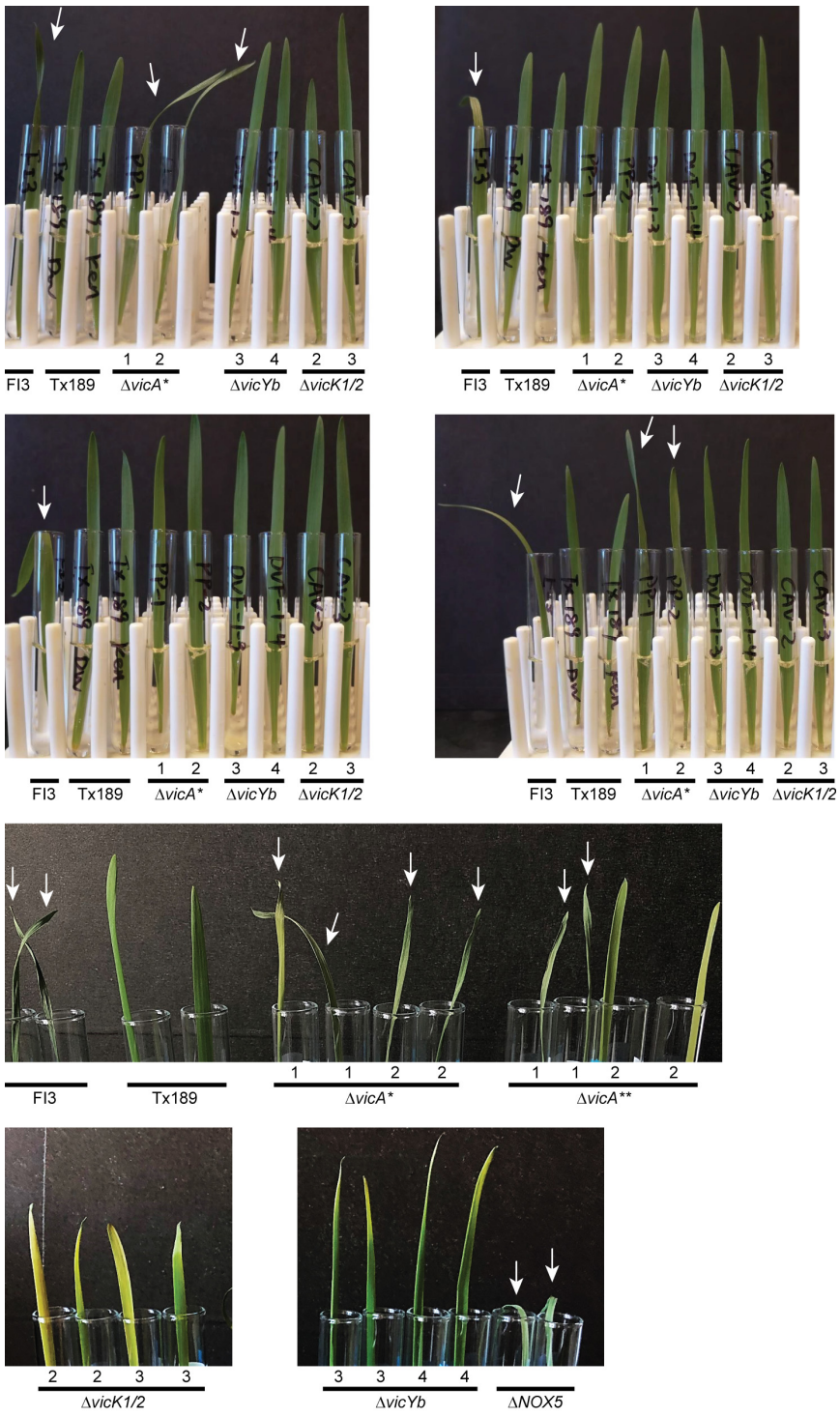

Figure S5. Replicates (includes replicates from Fig. 3B) of victorin toxicity assay on susceptible oat cultivar (Fulgrain) leaves with undiluted culture filtrate from different *C. victoriae* strains. Arrows indicate leaf wilting. Numbers above strain names indicate independent transformants (Table S5). Multiple tubes of the same strain name without numbering are biological replicates of the same strains.

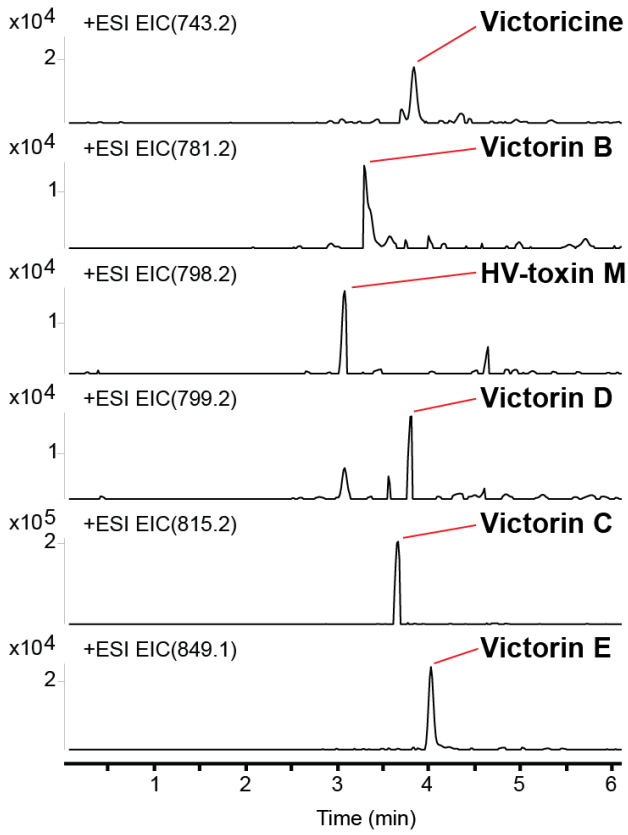

Figure S6. LC-MS analysis of victorin production of *C. victoriae* strain Δ*NOX5*. EICs correspond to $[M+H]^+$ masses of victorin B, C, D, E, HV-toxin M and victoricine.

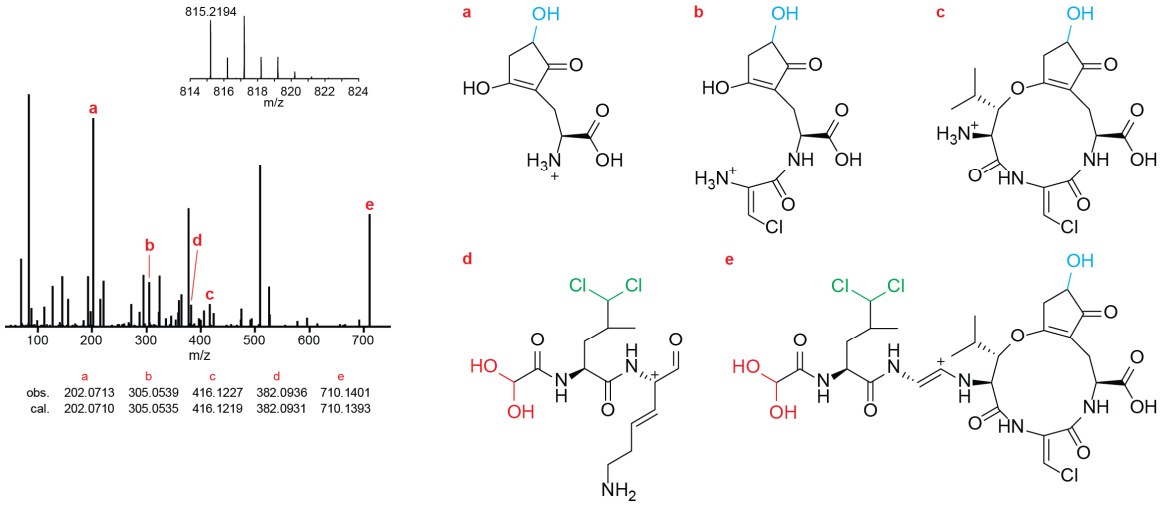

Figure S7. MS^2 analysis of the victorin C standard. MS^1 and MS^2 spectra of the $[M+H]^+$ ion corresponding to the mass of victorin C, with proposed structures of select fragments.

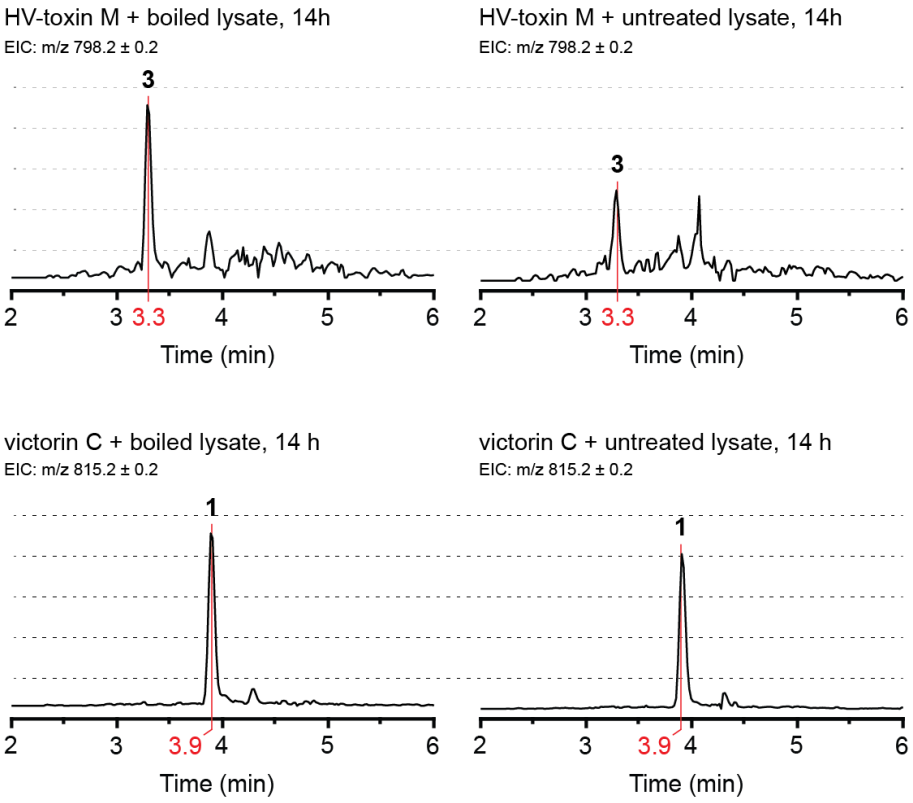

Figure S8. Investigation of consumption of HV-toxin M (**3**) and victorin C (**1**) by native *A. nidulans* enzymes. LC-MS analysis of **3** or **1** incubated with *A. nidulans* cell-free lysate boiled or untreated for 14 h. EICs correspond to $[M+H]^+$ masses of **3** and **1**.

Table S1. JGI mycocosm gene IDs of genes mentioned in this study.

C. victoriae [a]	JGI gene ID
A1	32336
CYP1	109554
K1	21377
NOX5	43041
Pa	116260
Pb	116699
R	43172
T	116826
Ya	115485
Yb	116011
Yc	116867
Yu	21381
Yv1	117381
Yv2	117381
Yw1	63600
Yw2	70699
Yx1	117098
Yx2	117098
Yx3	117098
Yz	32161
Yy1	117222
Yy2	117222

A. montagnei [b]	JGI gene ID
A	35111
R	119888
T	719332
Ya	35105
Yb	106157
Yc	106159
Yd	106160
Ye	50398
Yx	106163
Yy	147907
Yz	106167

C. eremochloae [c]	JGI gene ID
A	667032
K	542021
L	667044
R	662877
T	632321
Ya	651177
Yb	622198
Yc	622199
Yd	622202
Ye	622203
Yy	622192
Yz	622193

[a] JGI mycocosm portal: Cocvi1
[b] JGI mycocosm portal: Apimo1
[c] JGI mycocosm portal: Coler1

Table S2. Amino acid sequence identity between proteins assumed to be involved in victorin biosynthesis and proteins from *A. montagnei* and *C. eremochloae* homologous putative RiPP clusters, based on global individual alignments. For each putative victorin biosynthesis protein, the single best match from *A. montagnei* and *C. eremochloae* homologous putative RiPP clusters is shown. Only sequence identities over 30% are listed. For *C. victoriae* protein duplicates, only one representative protein sequence identity is listed.

C. victoriae	***A. montagnei***	**sequence identity [%]**	***C. eremochloae***	**sequence identity [%]**
A1	A	44.2	A	32.3
K1	-	-	K	39.1
CYP1	-	-	L	44.3
T	T	53.5	T	51.3
Ya	Ya	52.1	Ye	57.2
Yb	Ye	47.4	Ya	47.2
Yc	Yd	34.1	Yb	30.9
Yw1	Yy	56.8	Yz	58.5
Yx1	Yz	33.2	-	-
Yz	Yc	35.1	Yc	33.5

Table S3. Amino acid identity in percentage based on global individual alignments of VicY proteins with UstY (shown to be involved in ustiloxin biosynthesis [23, 24]) and AprY (shown to be involved in asperipin-2a biosynthesis [25, 26]) proteins.

	AprY	UstYa	UstYb
VicYa	19.9	24.3	26.1
VicYb	20.2	22.8	20.6
VicYc	20.6	19.5	16.9
VicYu	14.6	18	14.5
VicYv1	16.7	12	16.1
VicYv2	15	13.2	15.3
VicYw1	15.9	15.2	15.2
VicYw2	17.3	15.9	16
VicYx1	14.2	16.4	16.8
VicYx2	14.1	16	16.6
VicYx3	14.8	20.6	16.7
VicYy1	13.2	14.2	16.6
VicYy2	14.2	16.4	16.5
VicYz	17.7	17.9	17.5

Table S4. Amino acid identity in percentage of VicY proteins based on global multiple alignment.

	VicYa	VicYb	VicYc	VicYu	VicYv1	VicYv2	VicYw1	VicYw2	VicYx1	VicYx2	VicYx3	VicYy1[a]	VicYy2[a]	VicYz
VicYa		13	13.5	8.2	10.6	10.3	10.5	10.5	12	12.9	13	10.9	13.3	10.3
VicYb	13		23	9.5	12.3	10.9	12.3	12.3	10.2	10.3	9.9	10	12.5	12.4
VicYc	13.5	23		7.4	11.3	10.1	9.1	9.4	9.1	9.7	9.9	10	10.4	14.1
VicYu	8.2	9.5	7.4		3.9	3.6	5.7	5.9	6.3	6.1	5.5	5.7	7	7.3
VicYv1	10.6	12.3	11.3	3.9		99.3	16.8	16.3	12.7	14	14.4	20.6	20.8	14.4
VicYv2	10.3	10.9	10.1	3.6	99.3		15.9	15.5	11.9	13	13.3	20.1	20.4	15
VicYw1	10.5	12.3	9.1	5.7	16.8	15.9		93.6	18.1	17.8	18.9	14.7	19.1	18.1
VicYw2	10.5	12.3	9.4	5.9	16.3	15.5	93.6		18.1	17.8	18.9	14.3	17.8	18.6
VicYx1	12	10.2	9.1	6.3	12.7	11.9	18.1	18.1		86.6	84.4	14.9	15.8	15
VicYx2	12.9	10.3	9.7	6.1	14	13	17.8	17.8	86.6		82.2	15.9	15.2	14.3
VicYx3	13	9.9	9.9	5.5	14.4	13.3	18.9	18.9	84.4	82.2		15.7	15.8	16.6
VicYy1[a]	10.9	10	10	5.7	20.6	20.1	14.7	14.3	14.9	15.9	15.7		69.2	21.8
VicYy2[a]	13.3	12.5	10.4	7	20.8	20.4	19.1	17.8	15.8	15.2	15.8	69.2		22.8
VicYz	10.3	12.4	14.1	7.3	14.4	15	18.1	18.6	15	14.3	16.6	21.8	22.8	

[a] VicYy1/2 have been grouped as duplicates despite a protein sequence identity of only 69.2% due to a >99% nucleotide sequence percentage identity.

Table S5. Strains used in this study.

Strain	Lab strain designation	Genotype/Phenotype	Comments	Reference
Cochliobolus victoriae FI3	FI3	*MAT1-2*; Victorin+	Wild type field isolate.	[27]
C. victoriae Tx189	Tx189	*MAT1-2*; Victorin-	*C. victoriae* strain HvW, REMI [28] mutant.	[29]
C. victoriae FI3 Δ*vicA**-1	ΔPP-1	*MAT1-2*; *hygB*^{R}	Deletion of one copy of *vicA1/2/3*. Referred to as Δ*vicA** in the main text.	This study
C. victoriae FI3 Δ*vicA**-2	ΔPP-2	*MAT1-2*; *hygB*^{R}	Deletion of one copy of *vicA1/2/3.* Referred to as Δ*vicA** in the main text.	This study
C. victoriae FI3 Δ*vicA***-1	ΔPP-2-13	*MAT1-2*; *hygB*^{R}; *gen*^{R}	Deletion of two copies of *vicA1/2/3.* Referred to as Δ*vicA*** in the main text.	This study
C. victoriae FI3 Δ*vicA***-2	ΔPP-2-3-1	*MAT1-2*; *hygB*^{R}; *gen*^{R}	Deletion of two copies of *vicA1/2/3.* Referred to as Δ*vicA*** in the main text.	This study
C. victoriae FI3 Δ*vicYb*-3	ΔDUF-1-3	*MAT1-2*; *hygB*^{R}	Deletion of *vicYb*.	This study
C. victoriae FI3 Δ*vicYb*-4	ΔDUF-1-4	*MAT1-2*; *hygB*^{R}	Deletion of *vicYb*.	This study
C. victoriae FI3 Δ*vicYb*-9	ΔDUF-1-9	*MAT1-2*; *hygB*^{R}	Deletion of *vicYb*.	This study
C. victoriae FI3 Δ*vicK1/2*-2	ΔCAO-2	*MAT1-2*; *hygB*^{R}	Deletion of both copies of *vicK1/2*.	This study
C. victoriae FI3 Δ*vicK1/2*-3	ΔCAO-3	*MAT1-2*; *hygB*^{R}	Deletion of both copies of *vicK1/2*.	This study
C. victoriae FI3 Δ*NOX5*	ΔNAPDH1	*MAT1-2*; *hygB*^{R}	Deletion of *NOX5*.	This study

Aspergillus nidulans LO8030	pyroA4, riboB2, pyrG89, nkuA::argB, sterigmatocystin cluster (AN7804-AN7825)Δ, emericellamide cluster (AN2545-AN2549)Δ, asperfuranone cluster (AN1039-AN1029)Δ, monodictyphenone cluster (AN10023-AN10021)Δ, terrequinone cluster (AN8512-AN8520)Δ, austinol cluster part 1 (AN8379-AN8384)Δ, austinol cluster part 2 (AN9246-AN9259)Δ, F9775 cluster (AN7906-AN7915)Δ, asperthecin cluster (AN6000-AN6002)Δ	Used as host for heterologous expression of VicK.	[30]

Table S6. Primers used in this study.

Primer	Sequence 5' to 3'	Description	Size of PCR product (kb)	Purpose
XZ36	GTTTTCTGGCGATTCGTTGT	5' flanking region of *vicA1/2/3* (first round), forward primer (F1)	0.79	Deletion of *vicA* (first round)
XZ37	TCCTGTGTGAAATTGTTATCCGCT TGAATAGGGTGGATGCCAAT	5' flanking region of *vicA1/2/3* (first round), reverse primer with *hygB* gene tail (R1)		
XZ38	GTCGTGACTGGGAAAACCCTGGC GAAGTTCTTGCTGACGGGTGT	3' flanking region of *vicA1/2/3* (first round), forward primer with *hygB* gene tail (F2)	0.65	
XZ39	GTTAACGTGCGGGATCAGTT	3'flanking region of *vicA1/2/3* (first round), reverse primer (R2)		
M13R	AGCGGATAACAATTTCACACAGGA	Forward primer to amplify *hygB*	2.5	
M13F	CGCCAGGGTTTTCCCAGTCACGA C	Reverse primer to amplify *hygB*		
NLC37	GGATGCCTCCGCTCGAAGTA	*hygB*, reverse primer	2.0	*vicA* (first round) deletion verification
ZL25	GCTATACTCACCTGGTCTCG	Upstream verification forward primer of *vicA1/2/3* (first round), pair with NLC37 (U)		
NLC38	CGTTGCAAGACCTGCCTGAA	*hygB*, forward primer	3.1	
ZL26	GAGGCAGCGACGATTACTATC	Downstream verification reverse primer of *vicA1/2/3* (first round), pair with NLC38 (D)		
PP-F	AGCGGATCCATCCTTCTTTT	Forward primer to detect *vicA1/2/3* (F)	0.12	
PP-R	CAGGCTCAACAGATGTCGTTT	Reverse primer to detect *vicA1/2/3* (R)		
DUF1-U-F	GGAGCATGCATTTCTCTACGA	5' flanking region of *vicYb,* forward primer (F1)	0.7	Deletion of *vicYb*
DUF1-U-R	TCCTGTGTGAAATTGTTATCCGCT TGGTATCAAAAGAAAAACAACTGA A	5' flanking region of *vicYb,* reverse		

		primer with *hygB* gene tail (R1)		
DUF1-D-F	GTCGTGACTGGGAAAACCCTGGC GTGCTACGAGCAGCAGCTAAA	3' flanking region of *vicYb,* forward primer with *hygB* gene tail (F2)	0.85	
DUF1-D-R	ATGGTGGAGCTGATTTCTGG	3'flanking region of *vicYb,* reverse primer (R2)		
M13R	AGCGGATAACAATTTCACACAGGA	As above	2.5	
M13F	CGCCAGGGTTTTCCCAGTCACGA C	As above		
NLC37	GGATGCCTCCGCTCGAAGTA	As above	2.1	*vicYb* deletion verification
XZ22	ACAACGCGTGGATAGAAACA	Upstream verification forward primer of *vicYb*, pair with NLC37 (U)		
NLC38	CGTTGCAAGACCTGCCTGAA	As above	2.9	
XZ23	CGGTATATCGCCGTTCAACT	Downstream verification reverse primer of *vicYb*, pair with NLC38 (D)		
XZ20	CGGTATGCTCATCGTCCTTT	Forward primer to amplify *vicYb* (F)	0.64	
XZ21	CATTGATCAGCCTGTCGTAA	Reverse primer to amplify *vicYb* (R)		
CAU-U-F	CTAGAGATGAAGGCCCTGGA	5' flanking region of *vicK1/2,* forward primer (F1)	0.62	Deletion of *vicK1/2*
CAU-U-R	TCCTGTGTGAAATTGTTATCCGCT ATCGGCACTGATAGGTTTGG	5' flanking region of *vicK1/2,* reverse primer with *hygB* gene tail (R1)		
CAU-D-F	GTCGTGACTGGGAAAACCCTGGC GGAGAAGGAGTGCAGGTTTGG	3' flanking region of *vicK1/2,* forward primer with *hygB* gene tail (F2)	0.56	
CAU-D-R	GGTTTTCGCGGATGAAGTAA	3' flanking region of *vicK1/2,* reverse primer (R2)		
M13R	AGCGGATAACAATTTCACACAGGA	As above	2.5	
M13F	CGCCAGGGTTTTCCCAGTCACGA C	As above		
NLC37	GGATGCCTCCGCTCGAAGTA	As above	1.9	*vicK1/2* deletion verification
XZ34	CGCAAACTAGCAAAAGCGTA	Upstream verification forward primer of *vicK1/2*, pair with NLC37 (U)		
NLC38	CGTTGCAAGACCTGCCTGAA	As above	2.8	
XZ35	GTATAGCGAACCCCCGTGTA	Downstream verification reverse		

		primer of *vicK1/2*, pair with NLC38 (D)		
XZ32	GCGTTCCTTCCACAGCTAAG	Forward primer to amplify *vicK1/2* (F)	0.64	
XZ33	AAGGGCTTCTTGGAGGGATA	Reverse primer to amplify *vicK1/2* (R)		
NO-5-F	CGGAGATATGAGGGCTGATG	5' flanking region of *NOX5,* forward primer (F1)	0.81	Deletion of *NOX5*
NO-5-R	TCCTGTGTGAAATTGTTATCCGCT CGAGCAACTGCAATCCTAAA	5' flanking region of *NOX5,* reverse primer with *hygB* gene tail (R1)		
NO-3-F	GTCGTGACTGGGAAAACCCTGGC GCCTGTTACGAACCTGAAAGGA	3' flanking region of *NOX5,* forward primer with *hygB* gene tail (F2)	0.83	
NO-3-R	TTGGCTGTATTTGTGCTGATG	3'flanking region of *NOX5,* reverse primer (R2)		
M13R	AGCGGATAACAATTTCACACAGGA	As above	2.5	
M13F	CGCCAGGGTTTTCCCAGTCACGA C	As above		
NLC37	GGATGCCTCCGCTCGAAGTA	As above	2.3	*NOX5* deletion verification
XZ26	GCCAAGTATTAGCGCAAGGT	Upstream verification forward primer of *NOX5*, pair with NLC37 (U)		
NLC38	CGTTGCAAGACCTGCCTGAA	As above	2.9	
XZ27	TCAAAACCTCTACCGGCATC	Downstream verification reverse primer of *NOX5*, pair with NLC38 (D)		
XZ24	CAGGGTACGGTACAGCGAAT	Forward primer to amplify *NOX5* (F)	0.78	
XZ25	GTCCTTCCGGACCACTAACA	Reverse primer to amplify *NOX5* (R)		
XZ57	AAGATATTGTTAGCGGCTTTGA	5' flanking region of *vicA1/2/3* (second round), forward primer (F1)	0.25	Deletion of *vicA1/2/3* (second copy)
XZ58	CACTGGAACAACTGGCATGGCTAA AGCCTGAAGAGCAAAA	5' flanking region of *vicA1/2/3* (second round), reverse primer with *nptII* gene tail (R1)		
XZ59	CAGGTACACTTGTTTAGAGGTGCG TAGGAGAGCATGTATGGA	3' flanking region of *vicA1/2/3* (second round), forward primer with *nptII* gene tail (F2)	0.21	
XZ60	TGAAGATGAGGTGATGCAATAAA	3'flanking region of *vicA1/2/3* (second		

		round), reverse primer (R2)		
XZ57	AAGATATTGTTAGCGGCTTTGA	Upstream verification forward primer of *vicA1/2/3* (second round), pair with DW70 (U)	3.0	*vicA1/2/3* (second copy) deletion verification
DW70	ACCTCTAAACAAGTGTACCTG	As above		
ZL22	AGTGAGCAACACAAGTGAGC	Downstream verification reverse primer of *vicA1/2/3* (second round), pair with DW69 (D)	3.9	
DW69	CATGCCAGTTGTTCCAGTG	As above		
PalcS-vicCOx-F	CAAAGCATTGAGCCCAGAAACAGCAGAAGCGGCCATGAAGCTATTTCTGCTCTTTACGTT	Amplification of *vicK1/2* with overhangs for insertion into NotI site of pYFAC-pyrG via Gibson Assembly	2.5	Assembly of pYFAC-pyrG-*vicK1/2* for heterologous expression of VicK under *alcS* promotor in *A. nidulans* LO8030
T1-vicCOx-2R	TCTACAATCAATTCAGGCCGTATTCAGGGCGGCCTGACTGGCGATATGTCTGACTAAC			

SI References

1. S. Koren *et al.*, Canu: Scalable and accurate long-read assembly via adaptive k-mer weighting and repeat separation. *Genome Res.* **27**, 722-736 (2017).
2. R. Vaser, I. Sovic, N. Nagarajan, M. Sikic, Fast and accurate *de novo* genome assembly from long uncorrected reads. *Genome Res.* **27**, 737-746 (2017).
3. B.J. Walker *et al.*, Pilon: An integrated tool for comprehensive microbial variant detection and genome assembly improvement. *PLoS One*. **9**, e112963 (2014).
4. L. Guy, J.R. Kultima, S.G. Andersson, genoPlotR: Comparative gene and genome visualization in R. *Bioinformatics*. **26**, 2334-5 (2010).
5. H. Quesneville *et al.*, Combined evidence annotation of transposable elements in genome sequences. *PLoS Comput. Biol.* **1**, 166-75 (2005).
6. T. Flutre, E. Duprat, C. Feuillet, H. Quesneville, Considering transposable element diversification in *de novo* annotation approaches. *PLoS One*. **6**, e16526 (2011).
7. M. Stanke, R. Steinkamp, S. Waack, B. Morgenstern, AUGUSTUS: A web server for gene finding in eukaryotes. *Nucleic Acids Res.* **32**, W309-W312 (2004).
8. J.J.A. Armenteros *et al.*, SignalP 5.0 improves signal peptide predictions using deep neural networks. *Nat. Biotechnol.* **37**, 420-+ (2019).
9. N.L. Catlett, B.-N. Lee, O.C. Yoder, B.G. Turgeon, Split-marker recombination for efficient targeted deletion of fungal genes. *Fungal Genetics Reports*. **50** (2003).
10. B.G. Turgeon, B. Condon, J.Y. Liu, N. Zhang, Protoplast transformation of filamentous fungi. *Molecular and Cell Biology Methods for Fungi*. **638**, 3-19 (2010).
11. S.W. Lu *et al.*, Tagged mutations at the *Tox1* locus of *Cochliobolus heterostrophus* by restriction enzyme-mediated integration. *Proc. Natl. Acad. Sci. U. S. A.* **91**, 12649-12653 (1994).
12. D.L. Wu, S. Oide, N. Zhang, M.Y. Choi, B.G. Turgeon, ChLae1 and ChVel1 regulate T-toxin production, virulence, oxidative stress response, and development of the maize pathogen *Cochliobolus heterostrophus. PLoS Pathog.* **8** (2012).
13. P. Inderbitzin, T. Asvarak, B.G. Turgeon, Six new genes required for production of T-toxin, a polyketide determinant of high virulence of *Cochliobolus heterostrophus* to maize. *Mol. Plant. Microbe Interact.* **23**, 458-472 (2010).
14. B.O. Keller, J. Suj, A.B. Young, R.M. Whittal, Interferences and contaminants encountered in modern mass spectrometry. *Anal. Chim. Acta*. **627**, 71-81 (2008).
15. J.Y. Hu *et al.*, Heterologous biosynthesis of elsinochrome A sheds light on the formation of the photosensitive perylenequinone system. *Chem. Sci.* **10**, 1457-1465 (2019).
16. D.G. Gibson *et al.*, Enzymatic assembly of DNA molecules up to several hundred kilobases. *Nat Methods*. **6**, 343-U41 (2009).
17. S. Fillinger, B. Felenbok, A newly identified gene cluster in *Aspergillus nidulans* comprises five novel genes localized in the *alc* region that are controlled both by the specific transactivator AlcR and the general carbon-catabolite repressor CreA. *Mol. Microbiol.* **20**, 475-488 (1996).
18. W.B. Yin *et al.*, Discovery of cryptic polyketide metabolites from dermatophytes using heterologous expression in *Aspergillus nidulans. Acs Synth Biol*. **2**, 629-634 (2013).
19. R.B. Pringle, R.P. Scheffer, Purification of selective toxin of *Periconia circinata. Phytopathology*. **53**, 785-& (1963).

20. J. Leach, B.R. Lang, O.C. Yoder, Methods for selection of mutants and *in vitro* culture of *Cochliobolus heterostrophus. J. Gen. Microbiol.* **128**, 1719-1729 (1982).
21. T.H. Tzeng, L.K. Lyngholm, C.F. Ford, C.R. Bronson, A restriction fragment length polymorphism map and electrophoretic karyotype of the fungal maize pathogen *Cochliobolus heterostrophus. Genetics*. **130**, 81-96 (1992).
22. J.Y. Hu, H. Li, Y.H. Chooi, Fungal dirigent protein controls the stereoselectivity of multicopper oxidase-catalyzed phenol coupling in viriditoxin biosynthesis*. J. Am. Chem. Soc.* **141**, 8068-8072 (2019).
23. Y. Ye *et al.*, Unveiling the biosynthetic pathway of the ribosomally synthesized and post-translationally modified peptide ustiloxin B in filamentous fungi*. Angew. Chem. Int. Ed. Engl.* **55**, 8072-5 (2016).
24. M. Umemura *et al.*, Characterization of the biosynthetic gene cluster for the ribosomally synthesized cyclic peptide ustiloxin B in *Aspergillus flavus. Fungal Genet. Biol.* **68**, 23-30 (2014).
25. Y. Ye *et al.*, Heterologous production of asperipin-2a: proposal for sequential oxidative macrocyclization by a fungi-specific DUF3328 oxidase*. Org. Biomol. Chem.* **17**, 39-43 (2019).
26. N. Nagano *et al.*, Class of cyclic ribosomal peptide synthetic genes in filamentous fungi*. Fungal Genet. Biol.* **86**, 58-70 (2016).
27. B.J. Condon *et al.*, Comparative genome structure, secondary metabolite, and effector coding capacity across *Cochliobolus pathogens. PLoS Genet.* **9**, e1003233 (2013).
28. R.H. Schiestl, T.D. Petes, Integration of DNA fragments by illegitimate recombination in *Saccharomyces cerevisiae. Proc. Natl. Acad. Sci. U. S. A.* **88**, 7585-7589 (1991).
29. A.C.L. Churchill, S. Lu, B. Turgeon, O.C. Yoder, V. Macko, Victorin-deficient REMI mutants of *Cochliobolus victoriae* demonstrate a requirement for victorin in pathogenesis*. Abstracts of the 18th Fungal Genetics Conference*, (1995).
30. Y.M. Chiang *et al.*, Development of genetic dereplication strains in *Aspergillus nidulans* results in the discovery of aspercryptin*. Angew. Chem. Int. Ed. Engl.* **55**, 1662-1665 (2016).